5.2 Fission Level Densities

Coordinator: V.M. Maslov

Summary

Fission level densities (or fissioning nucleus level densities at fission saddle deformations) are required for statistical model calculations of actinide fission cross sections. Back-shifted Fermi-Gas Model, Constant Temperature Model and Generalized Superfluid Model (GSM) are widely used for the description of level densities at stable deformations. These models provide approximately identical level density description at excitations close to the neutron binding energy. It is at low excitation energies that they are discrepant, while this energy region is crucial for fission cross section calculations. A drawback of back-shifted Fermi gas model and traditional constant temperature model approaches is that it is difficult to include in a consistent way pair correlations, collective effects and shell effects. Pair, shell and collective properties of nucleus do not reduce just to the renormalization of level density parameter a, but influence the energy dependence of level densities. These effects turn out to be important because they seem to depend upon deformation of either equilibrium or saddle-point. These effects are easily introduced within GSM approach [5.28]. Fission barriers are another key ingredients involved in the fission cross section calculations. Fission level density and barrier parameters are strongly interdependent. This is the reason for including fission barrier parameters along with the fission level densities in the Starter File.

The recommended file is **maslov.dat** — fission barrier parameters. Recent version of actinide fission barrier data obtained in Obninsk (*obninsk.dat*) should only be considered as a guide for selection of initial parameters. These data are included in the Starter File, together with the fission barrier parameters recommended by CNDC (*beijing.dat*), for completeness.

5.2.1 Introduction

Fission level densities and fission barrier parameters are key ingredients of actinide fission calculations. The important point is that fission level density and barrier parameters are strongly interdependent. The level density of deformed nucleus depends on the collective properties, pair correlations, and shell structure of a nucleus. These effects are easily introduced within the framework of the Generalized Superfluid Model [5.28]. Data on neutron-induced fission cross sections provide a sound basis for extraction of fission barrier parameters and for modeling level density approach. We proceed within the full-scale Hauser-Feshbach theory, coupled channel optical model and double-humped fission barrier model [5.42]. This approach is supported by many experimental signatures which demonstrate the importance of the collective, pairing, and shell effects both at equilibrium and saddle deformation.

Total nuclear level density is represented as a product of quasi-particle and collective contributions. The collective contribution to the level density at a saddle point is defined by the order of symmetry of a saddle point, which can be adopted according to the calculations within the shell correction method, such as the ones by Howard and Möller [5.43]. These saddle asymmetries depend on Z and N of the fissioning nucleus.

The effect of the pair correlations on the level density was demonstrated in the measurements of statistical γ–decay spectra on even rare-earth nuclei [5.44, 5.45]. In case of even-even

fissioning nuclei step-like structure of the K_o^2 parameter, defining the angular anisotropy of fission fragments, is interpreted as being due to few-quasi-particle excitations. These excitations are essential for state density calculation at low intrinsic excitation energies. Contrary to the fission cross section, the structure observed in the behavior of the K_o^2 parameter, is virtually insensitive to the detailed shape of the fission level density. It was demonstrated that the observed irregularities in neutron-induced fission cross sections can be attributed to the interplay of few-quasi-particle excitations in the level density of fissioning and residual nuclei [5.46, 5.47].

The shell structure effects are introduced through the dependence of the level density $a-$parameter on the excitation energy. Damping of the shell effects influences the shape of first-chance fission cross section at excitation energies above fission threshold. The impact of pairing correlations and of collective and shell effects, on the calculated fission cross sections depends on the excitation energy [5.48, 5.49].

It was demonstrated that the sophisticated level density approach, involving pair, shell and collective effects, is unavoidable.

5.2.2 Fission Level Densities

In the adiabatic approximation the total nuclear level density $\rho(U, J, \pi)$ is represented as a product of quasi-particle and collective contributions,

$$\rho(U, J, \pi) = K_{rot}(U, J) K_{vib}(U) \rho_{qp}(U, J, \pi), \tag{5.32}$$

where $\rho_{qp}(U, J, \pi)$ is the quasi-particle level density, and $K_{rot}(U, J)$ and $K_{vib}(U)$ are rotational and vibrational enhancement factors. The collective contribution to the level density of a deformed nucleus is defined by the symmetry order of nuclear deformation. The actinide nuclei equilibrium deformation is axially symmetric. The symmetry order of nuclear shape at inner and outer saddle point is adopted according to the calculations performed using shell correction method [5.43].

Level densities at equilibrium deformations should reproduce both: (i) the average neutron resonance spacings and (ii) the observed cumulative number of discrete levels $N^{exp}(U)$ (see previous Chapter). In the latter case, GSM model fails to describe the cumulative number of low-lying levels without introduction of the additional shift in the excitation energy δ_{shift}. Therefore, level densities at low excitation energies (i.e. just above the last discrete level where $N^{exp}(U) \sim N^{theor}(U)$) a modified constant temperature model is applied. The constant temperature approximation

$$\rho(U) = dN(U)/dU = T^{-1} \exp((U - U_o)/T), \tag{5.33}$$

is extrapolated up to the matching point U_c above which the GSM model [5.28] is adopted. The following condition is imposed:

$$U_c = U_o - T \ln(T\rho(U_c)). \tag{5.34}$$

Here, the odd-even energy shift $U_o = -n\Delta$, where $\Delta = 12/\sqrt{A}$ is the pairing correlation function, A is a mass number, and $n = 0$ for even-even, 1 for odd and 2 for odd-odd nuclei. The value of nuclear temperature T is defined by the matching conditions at excitation energy U_c. The constant temperature model parameters for some actinides are given in Table 5.1.

The respective parameters for axially symmetric fissioning nucleus (nuclear temperature T_f and excitation energy shift U_{of}) are defined at the matching energy U_{cf}, which is assumed to be the same as for the equilibrium deformation (U_c). This is a fair approximation because for ground state deformations the U_c value is not very much sensitive to the value of the $a-$parameter. The

Table 5.1: Constant temperature model parameters.

Parameter	^{246}Cm	^{245}Cm	^{241}Am	^{242}Am
U_c, MeV	3.6	2.4	3.6	2.4
U_o, MeV	-0.0068	-0.65311	-0.96455	-1.6452
T, MeV	0.37326	0.36246	0.40723	0.39241

effects of non-axiality and mass asymmetry are included afterwards. At excitation energies above U_{cf} the GSM model [5.28] is applied.

The parameters of the level density model for the inner (outer) saddle points and equilibrium deformations are:

- main level density parameters a_f and a,
- shell corrections $\delta W_{fA(B)}$ and δW,
- pairing correlation functions Δ_f and Δ , at equilibrium deformations $\Delta_o = 12/\sqrt{A}$,
- quadrupole deformation ε,
- moment of inertia at zero temperature $\mathcal{I}_0/\hbar^2$

Values of these parameters for actinides are given in Table 5.2. Shell corrections for ground state deformations are calculated as $\delta W = M^{exp} - M^{MS}$, where M^{MS} denotes liquid drop mass (LDM), calculated with Myers-Swiatecki parameters [5.23], and M^{exp} is the experimental nuclear mass. Shell correction values at inner and outer saddle deformations $\delta W_{fA(B)}$ are taken from the comprehensive review by Bjornholm and Lynn [5.50]. Correlation function $\Delta_f = \Delta_o + \delta$ at saddle-point depends on a_f/a ratio, which is a function of $(\delta W_f - \delta W)$.

Table 5.2: Level density parameters for fission and neutron emission channels in actinide nuclei.

Parameter	inner saddle (A)	outer saddle (B)	neutron channel
δW, MeV	2.5**	0.6	LDM
Δ, MeV	$\Delta_o + \delta$ *	$\Delta_o + \delta$ *	Δ_o
ε	0.6	0.8	0.24
$\mathcal{I}_0/\hbar^2$, MeV^{-1}	100	200	73

**) for axially asymmetric deformations, 1.5 MeV for axially symmetric deformations;
*) $\delta = \Delta_f - \Delta$ value is defined by fitting fission cross section in the plateau region.

Values of the $\tilde{a}-$parameter are determined by fitting neutron resonance spacings $\langle D_{obs} \rangle$. These, along with the $s-$wave neutron strength function $\langle S_o \rangle$, are obtained taking into account the correction for resonances missing due to their weakness and/or to poor experimental resolution [5.51]. Essentially, these values are consistent with those recommended for the RIPL Starter File (see file *obninsk.dat*). The shell correction dependence of $a-$parameter is defined using the following equation [5.28]:

$$a(U) = \begin{cases} \tilde{a}(1 + \delta W f(U - E_{cond})/(U - E_{cond})), & U > U_{cr} = 0.47 a_{cr} \Delta^2 - n\Delta \\ a(U_{cr}) = a_{cr} & U \leq U_{cr} = 0.47 a_{cr} \Delta^2 - n\Delta, \end{cases} \quad (5.35)$$

where $n = 0$, 1, 2 for even-even, odd-A and odd-odd nuclei, respectively; $f(x) = 1 - \exp(-\gamma x)$ is the dimensionless function describing damping of the shell effects; condensation energy $E_{cond} =$

$0.152a_{cr}\Delta^2$, where Δ is the correlation function; $\tilde{a}$ is the asymptotic a-parameter value at high excitation energies. It is assumed that $\tilde{a}$-values for equilibrium and saddle deformations are identical.

This means that the complete expression for the constant temperature approach to the total level density reads

$$\rho(U) = K_{rot}(U)K_{vib}(U)\frac{\omega_{qp}(U)}{\sqrt{2\pi}\sigma} = T^{-1}\exp((U-U_o)/T). \tag{5.36}$$

The quasi-particle state densities $\omega_{qp}(U)$ are renormalized at excitation energies $U < U_c$. Here, $\sigma^2 = \mathcal{I}_{||}\ t$ is the spin distribution parameter, t is thermodynamic temperature, the parallel moment of inertia $\mathcal{I}_{||} = 6/\pi^2 < m^2 > (1 - 2/3\varepsilon)$, where $< m^2 >$ is the average value of the squared projection of the angular momentum of the single-particle states, and ε is quadrupole deformation parameter.

For deformed axially symmetric nucleus it is assumed

$$K_{rot}(U) = \sigma_\perp^2 = \mathcal{I}_\perp t = 0.4mr_o^2\hbar^{-2}(1 + 1/3\varepsilon), \tag{5.37}$$

where $\sigma_\perp^2$ is the spin cutoff parameter, $\mathcal{I}_\perp$ is the nuclear moment of inertia (perpendicular to the symmetry axis). $\mathcal{I}_\perp$ is taken equal to the rigid-body value at high excitation energies (at which pairing correlations are destroyed), while experimental value is adopted at zero temperature. In the intermediate range, values interpolated using the GSM equations [5.28] are used.

For $\gamma-$asymmetric nuclides the rotational enhancement factor is

$$K_{rot}(U) = 2\sqrt{2\pi}\sigma_\perp^2\sigma. \tag{5.38}$$

The closed-form expressions for the thermodynamic temperature and other relevant equations needed to calculate $\rho(U, J, \pi)$ are provided by the GSM model [5.28]. Mass asymmetry increases level densities by a factor of 2.

The quasi-particle level density $\rho_{qp}(U, J, \pi)$ is defined as

$$\rho_{qp}(U, J, \pi) = \frac{(2J+1)\omega_{qp}(U)}{4\sqrt{2\pi}\sigma_\perp^2\sigma}\exp\left(-\frac{J(J+1)}{2\sigma_\perp^2}\right). \tag{5.39}$$

Few-quasi-particle effects, due to pairing correlations, are essential for state density calculation at low intrinsic excitation energies of recently. The section was shown to two-quasi-particle configurations ^{238}Pu [5.52]. The same effect is observed in the ^{238} U(n,γ) data due to (n,γ n') reaction competition [5.53]. It was demonstrated that effects are important for reproducing fission cross sections below ~2 MeV incident neutron energy [5.46, 5.54]. Observed irregularities in neutron-induced fission cross be attributed to the interplay of few-quasiparticle the level density of fissioning and residual nuclei. $n-$quasiparticle state densities, which sum-up to the intrinsic state density of quasiparticle excitations can be estimated using Bose-gas model predictions [5.52, 5.55]

$$\omega_{qp}(U) = \sum_n \omega_{nqp}(U) = \sum_n \frac{g^n(U-U_n)^{n-1}}{((n/2)!)^2(n-1)!}, \tag{5.40}$$

where $g = 6a_{cr}/\pi^2$ is a single-particle state density at the Fermi surface, and n is the number of quasi-particles. This equation provides energies. Partial state densities $\omega_{nqp}(U)$ depend critically on the excitation of the n-quasi-particle odd-A nuclei, n = 2, 4, ... for even-even and odd-odd

nuclei). The discrete character of few-quasi-particle excitations is unimportant only in the case of odd-odd nuclei. The values of U_n are given by [5.55]

$$U_n = \begin{cases} E_{cond}(3.23n/n_{cr} - 1.57n^2/n_{cr}^2), & \text{if } n < 0.446\ n_{cr} \\ E_{cond}(1 + 0.627n^2/n_{cr}^2), & \text{if } n \geq 0.446\ n_{cr}. \end{cases} \tag{5.41}$$

Here, $n_{cr} = 12/\pi^2(\ln 2)gt_{cr}$, $t_{cr} = 0.571\Delta$ is a critical temperature, and $E_{cond} = 0.152a_{cr}\Delta^2 - m\Delta$ is a condensation energy (with m=0, 1, 2 for even-even, odd-A and odd-odd nuclides, respectively). Eq.5.41 takes into account the energy dependence of the correlation function $\Delta(U)$ and a modified Pauli correction to the excitation energy. The angular momentum distribution parameter σ^2 can be written as

$$\sigma^2 = \sum_n n\langle m^2\rangle\omega_{nqp}(U) / \sum_n \omega_{nqp}(U), \tag{5.42}$$

where $\langle m^2\rangle = 0.24A^{2/3}$ is the average value of the squared projection of the angular momentum of the single-particle states on the symmetry axis.

The pairing is weakened by excitation of few-quasi-particle states. Actually, only the lowest-number quasi-particle states (n =2 for even nuclei and n =1 for odd nuclei) lead to the pronounced structure in the total level density for actinide nuclei [5.52]. In the case of even-even nuclei, at excitations below four-quasi-particle excitation threshold, the intrinsic state density $\omega_2(U)$ can be represented by Eq. (5.40) modified with a Woods-Saxon type factor:

$$\omega_2(U) = g^2(U_4 - U_2 - \alpha)\left[1 + \exp((U_2 - U + \beta)/\gamma)\right]^{-1}. \tag{5.43}$$

This estimate of $\omega_2(U)$ was obtained by modeling the structure of ^{238}Pu intrinsic state density in order to interpret observed step-like structure in the ^{239}Pu(n,2n) reaction near the threshold [5.52].

To avoid the use Bose-gas equations (Eq. (5.40)) for the intrinsic state densities, the step-like behavior can be simulated within the constant temperature model. At excitation energies above the pairing gap (i.e. $U > U_2$) but below the four-quasi-particle excitation threshold, the level density $\rho(U)$ of an axially symmetric fissioning nucleus is calculated as

$$\rho(U) = \rho(U_4 - \delta_4)/(1 + \exp(U_2 - U + \delta_a)/\delta_s). \tag{5.44}$$

This estimate almost coincides with the predictions of the Bose-gas model. The numerical values: δ_4 =0.5 MeV, $\delta_a = 0.1 \div 0.2$ MeV, $\delta_s = 0.1 \div 0.2$ MeV were extracted by fitting fission cross section data. Fission level density for even-even nuclide ^{234}U at outer saddle, as calculated within the current approach (Eq. (5.44)), are compared with the constant temperature model approximation on Fig. 5.7. Collective levels are used below the threshold for the 2-quasi-particle excitations (U_2). In case of axial symmetry at the inner saddle the band-heads spectra are similar to that at equilibrium deformation. In case of axial asymmetry at the inner saddle the 2^+ band-heads are sufficiently lowered. The position of negative parity band $K^\pi = 0^-$ at outer saddle is lowered due to mass asymmetry (see Table 5.3)

In the case of odd-even and even-odd nuclei the partial contributions $\omega_{nqp}(U)$ of $n-$quasiparticle states to the total intrinsic state density $\omega_{qp}(U)$ produce a distinct "jump" only below the 3-quasi-particle excitation threshold (U_3). The level density of the fissioning nucleus at excitations $U > U_3$ may be calculated introducing odd-even excitation energy shift: $\hat{U} = U + \Delta_f$, where Δ_f is the correlation function for the saddle point deformation. Nuclear level density $\rho(U)$ up to the 3-quasi-particle excitation threshold U_3 is actually independent on the excitation energy, since the intrinsic state density ($\omega_1 \sim g$) is constant. Therefore, level densities in this energy region can be written as

$$\rho(U) = T_f^{-1}\exp((U_3 + \Delta_f - U_o - \delta_3)/T_f) \sim \exp((\Delta_f - U_o)/T_f). \tag{5.45}$$

Table 5.3: Transition spectra band-heads of even-even nuclei.

inner saddle			outer saddle	
K^π	$E^{ax}_{K^\pi}$, MeV	$E^{nonax}_{K^\pi}$, MeV	K^π	E_{K^π}, MeV
0^+	0.0	0.0	0^+	0.0
2^+	0.5	0.1	2^+	0.5
0^-	0.4	0.4	0^-	0.2
1^-	0.4	0.4	1^-	0.5
2^+	0.5	0.5	2^+	
2^-	0.4	0.4	2^-	
0^+	0.8	0.8	0^+	
0^+	0.8	0.8	0^+	

Table 5.4: Transition spectra band-heads of Z-odd, N-even nuclei.

inner saddle		outer saddle	
K^π	E_{K^π}, MeV	K^π	E_{K^π}, MeV
$3/2^-$	0.0	$5/2^+$	0.0
$5/2^+$	0.140	$5/2^-$	0.0
$7/2^-$	0.180	$3/2^+$	0.08
$5/2^-$	0.180	$3/2^-$	0.08
		$1/2^+$	0.04
		$1/2^-$	0.04
		$1/2^+$	0.05
		$1/2^-$	0.05

Above the 3-quasi-particle states excitation threshold the constant temperature model is used. However, for the excitation energies between 3-quasi-particle and 5-quasi-particle excitation thresholds, the level density can be slightly increased, as compared with the constant temperature approximation:

$$\rho(U) = T_f^{-1} \exp((U - U_o + \delta_5)/T_f). \tag{5.46}$$

The discrete transition state spectra, for excitation energies up to 200 keV, can be constructed using one-quasi-particle states by Bolsterli *et al.* [5.56]. Each one-quasi-particle state in odd fissioning nucleus is assumed to have a rotational band built on it with a rotational constant, depending on the respective saddle-point deformation (see Tables 5.4i and 5.5). Due to the axial asymmetry at the inner saddle we additionally assume $(2J + 1)$ rotational levels for each J value. The positive parity bands $K^\pi = 1/2^+,\ 3/2^+,\ 5/2^+, \ldots$ at outer saddle are assumed to be doubly degenerated due to mass asymmetry [5.43]. The intrinsic 2-quasi-particle spectrum

Table 5.5: Transition spectra band-heads Z-even, N-odd nuclei.

inner saddle		outer saddle	
K^π	E_{K^π}, MeV	K^π	E_{K^π}, MeV
$1/2^+$	0.0	$1/2^+$	0.0
$5/2^+$	0.08	$1/2^-$	0.0
$1/2^-$	0.05	$3/2^+$	0.08
$3/2^-$	0.0	$3/2^-$	0.08
		$5/2^+$	0.0
		$5/2^-$	0.0

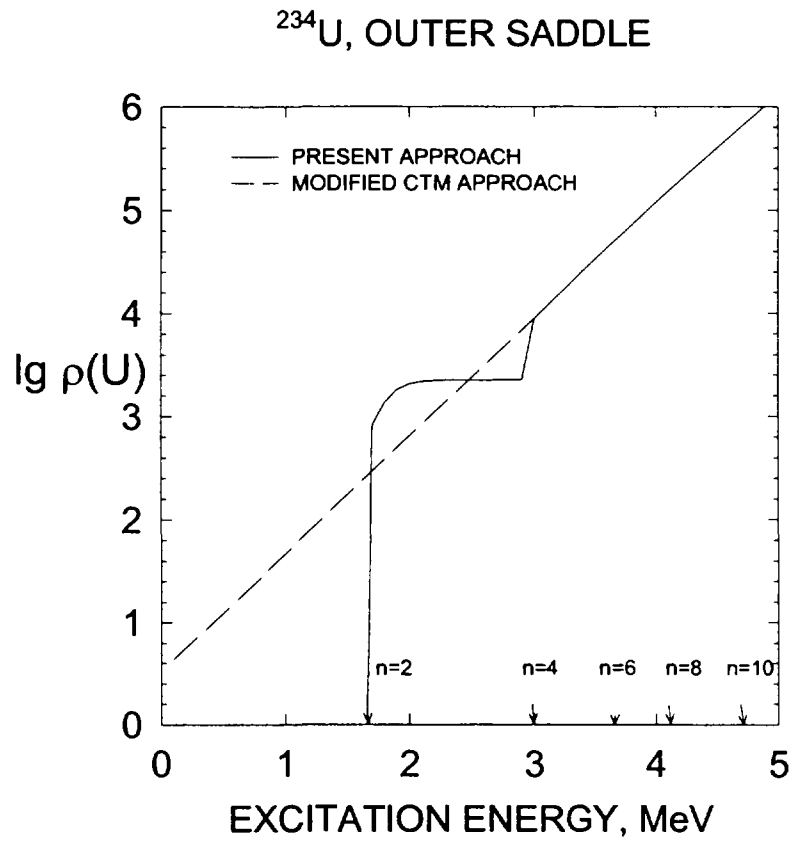

Figure 5.7: Level densities at outer saddle-point in ^{234}U. The arrows on the horizontal axis indicate excitation thresholds of even n−quasi-particle configurations.

of odd-odd nuclide ^{242}Am at equilibrium deformation can be obtained following Sood and Singh [5.57]. The expected location of still unobserved two-quasi-particle states was predicted (see Table 5.6). Using these intrinsic states as the band-head energies the rotational bands can be built in the same way as for Z-odd, N-even nuclei.

Table 5.6: Transition spectra band-heads of Z−odd, N−odd nuclei.

inner saddle		outer saddle	
K^π	E_{K^π}, MeV	K^π	E_{K^π}, MeV
1^-	0.0	1^-	0.0
0^-	0.044	0^-	0.044
5^-	0.049	5^-	0.049
6^-	0.170	6^-	0.170
1^-	0.220	1^-	0.220
3^-	0.242	$3-$	0.242
2^-	0.288	2^-	0.288

The values of δ_3 and δ_5 parameters can be defined by fitting fission cross section data. The level densities calculated with Eqs. (5.45) and (5.46) at the inner saddle-point of ^{239}Pu are shown on Fig. 5.8.

Adopting fission and total level densities modeling described above fission barrier parameters were extracted from the experimental neutron-induced fission cross sections on $^{232-238}$U, $^{238-244}$Pu, $^{241-243}$Am, and $^{242-248}$Cm targets [5.58-5.63]. Fission barrier parameters for Th, Pa,

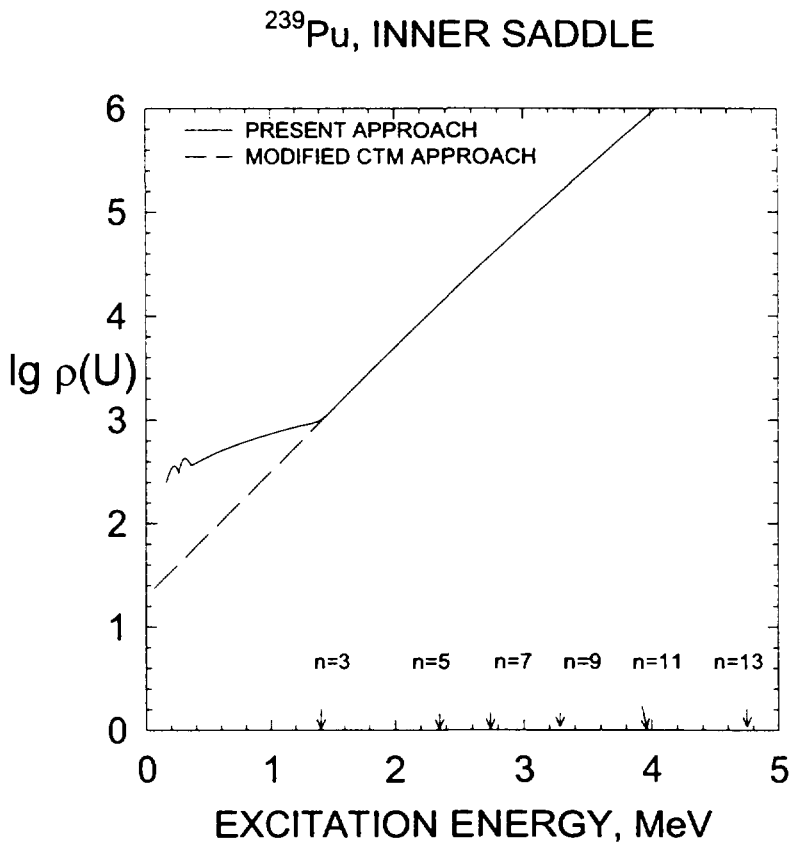

Figure 5.8: Level densities at inner saddle-point in ^{239}Pu. The arrows on the horizontal axis indicate excitation thresholds of odd $n-$quasi-particle configurations.

and Np nuclei were obtained essentially within the same approach [5.64–5.66]. In the latter case, however, the parameters should be treated as rather crude estimates, due to the more complex structure of fission barriers in Th and Pa as compared to the transuranium nuclei.

Fission barrier parameters: inner(A) and outer(B) barrier heights ($E_{fA(B)}$) and curvatures ($\hbar\omega_{A(B)}$) are given in Table 5.7. The symbol SYM denotes the symmetry of saddle point deformation. Comparison of the obtained results with the fission barriers determined by Smirenkin [5.67] shows the following: (i) for isotopes of uranium the agreement is rather good for outer fission barriers, while the isotopic dependencies for the inner barriers are similar, (ii) for Pu and Am the agreement is also good, except the americium outer barrier for neutron-deficient isotopes. It should be noted that the recommended barriers for neutron-deficient Am nuclei were determined from the analysis of the data for the ^{241}Am(n,f) reaction [5.59]. The largest discrepancies are observed in the case of outer barriers in Cm.

5.2.3 Conclusions and Recommendations

Recommended sophistication of the level density model, as compared to the conventional approaches, is needed in order to reproduce experimental data with the consistent level density and barrier parameters. It should be stressed, that the use of the recommended fission barriers also implies the use of the described approach to the level densities above the inner and outer saddle-points. The recommended fission barrier parameters are contained in **maslov.dat** file.

Table 5.7: Fission barrier parameters.

Nuclide	E_{fA},MeV	Sym.(A)	E_{fB},MeV	Sym.(B)	$\hbar\omega_A$,MeV	$\hbar\omega_B$,MeV	Δ_f,MeV
^{230}Th	6.1	S	6.8	MA	0.9	0.6	0.832
^{231}Th	6.0	S	6.7	MA	0.7	0.5	0.830
^{232}Th	5.8	S	6.7	MA	0.9	0.6	0.828
^{233}Th	5.1	S	6.65	MA	0.7	0.5	0.806
^{230}Pa	5.6	S	5.8	MA	0.6	0.4	0.802
^{231}Pa	5.5	S	5.5	MA	1.0	0.5	0.800
^{232}Pa	5.0	S	6.4	MA	0.6	0.4	0.828
^{233}Pa	5.7	S	5.8	MA	1.0	0.5	0.808
^{234}Pa	6.3	S	6.15	MA	0.6	0.4	0.806
^{231}U	4.4	S	5.5	MA	0.7	0.5	0.869
^{232}U	4.9	S	5.4	MA	0.9	0.6	0.848
^{233}U	4.35	S	5.55	MA	0.8	0.5	0.946
^{234}U	4.8	S	5.5	MA	0.9	0.6	0.889
^{235}U	5.25	S	6.0	MA	0.7	0.5	0.803
^{236}U	5.0	S	5.67	MA	0.9	0.6	0.833
^{237}U	6.4	GA	6.15	MA	0.7	0.5	0.809
^{238}U	6.3	GA	5.5	MA	1.0	0.6	0.818
^{239}U	6.45	GA	6.0	MA	0.7	0.5	0.816
^{236}Np	5.9	GA	5.4	MA	0.6	0.4	0.821
^{237}Np	6.0	GA	5.4	MA	1.0	0.5	0.819
^{238}Np	6.5	GA	5.75	MA	0.6	0.4	0.820
^{237}Pu	5.10	S	5.15	MA	0.7	0.5	0.799
^{238}Pu	5.6	S	5.1	MA	0.9	0.6	0.818
^{239}Pu	6.2	GA	5.7	MA	0.7	0.5	0.816
^{240}Pu	6.05	GA	5.15	MA	0.9	0.6	0.875
^{241}Pu	6.15	GA	5.50	MA	0.7	0.5	0.855
^{242}Pu	5.85	GA	5.05	MA	0.9	0.6	0.846
^{243}Pu	6.05	GA	5.45	MA	0.7	0.5	0.910
^{244}Pu	5.7	GA	4.85	MA	0.9	0.6	0.848
^{245}Pu	5.85	GA	5.25	MA	0.7	0.5	0.855
^{239}Am	6.00	GA	5.40	MA	0.8	0.5	0.776
^{240}Am	6.10	GA	6.00	MA	0.6	0.4	0.775
^{241}Am	6.00	GA	5.35	MA	0.8	0.5	0.773
^{242}Am	6.32	GA	5.78	MA	0.6	0.4	0.884
^{243}Am	6.40	GA	5.05	MA	1.0	0.5	0.770
^{244}Am	6.25	GA	5.9	MA	0.7	0.53	0.808
^{241}Cm	7.15	GA	5.5	MA	0.7	0.5	0.793
^{242}Cm	6.65	GA	5.0	MA	0.9	0.6	0.811
^{243}Cm	6.33	GA	5.4	MA	0.7	0.5	0.810
^{244}Cm	6.18	GA	5.10	MA	0.9	0.6	0.868
^{245}Cm	6.35	GA	5.45	MA	0.7	0.5	0.867
^{246}Cm	6.00	GA	4.80	MA	0.9	0.6	0.865
^{247}Cm	6.12	GA	5.10	MA	0.7	0.5	0.883
^{248}Cm	5.80	GA	4.80	MA	0.9	0.6	0.842
^{249}Cm	5.63	GA	4.95	MA	0.7	0.5	0.900

S - symmetric saddle point, GA - axially asymmetric saddle point, MA - mass asymmetric saddle point.